HHS Public Access

Author manuscript

Gastroenterology. Author manuscript; available in PMC 2021 February 01.

Published in final edited form as:

Gastroenterology. 2020 February ; 158(3): 583–597.e1. doi:10.1053/j.gastro.2019.10.040.

Isoforms of RNF128 Regulate the Stability of Mutant P53 in Barrett's Esophageal Cells

Dipankar Ray[1], **Paramita Ray**[1], **Daysha Ferrer-Torres**[2], **Zhuwen Wang**[2], **Derek Nancarrow**[2], **Hee-won Yoon**[2], **May San Martinho**[1], **Tonaye Hinton**[1], **Scott Owens**[3], **Dafydd Thomas**[3], **Hui Jiang**[4], **Theodore S. Lawrence**[1], **Jules Lin**[2], **Kiran Lagisetty**[2], **Andrew C. Chang**[2], **David G. Beer**[1,2]

[1]Department of Radiation Oncology, University of Michigan, Ann Arbor, Michigan

[2]Department of Surgery, Thoracic Surgery, University of Michigan, Ann Arbor, Michigan

[3]Department of Pathology, University of Michigan, Ann Arbor, Michigan

[4]Department of Biostatistics, University of Michigan, Ann Arbor, Michigan

Abstract

BACKGROUND & AIMS: Barrett's esophagus (BE) can progress to dysplasia and esophageal adenocarcinoma (EAC), accompanied by mutations in *TP53* that increase the stability of its product, p53. We analyzed BE tissues for messenger RNAs (mRNAs) that associate with BE progression and identified one that affects the stabilization of p53.

METHODS: We obtained 54 BE samples collected from patients with high-grade dysplasia (HGD) or esophageal adenocarcinoma (EAC), from 1992 through 2015, and performed RNA sequence analyses, including isoform-specific analyses. We performed reverse-transcription polymerase chain reaction analyses of 166 samples and immunohistochemical analyses of tissue microarrays that contained BE tissues from 100 patients with HGD or EAC and normal esophageal squamous mucosa (controls). Proteins were expressed from transfected plasmids or knocked down with small interfering RNAs in BE cells and analyzed by immunoblots and in immunoprecipitation and ubiquitin ligase assays. Athymic nude mice bearing EAC xenograft tumors (grown from OE-33 cells) were given intraperitoneal injections of simvastatin; tumor growth was monitored and tumors were collected and analyzed by immunoblotting for levels of RNF128, p53, and acetylated p53.

Correspondence Address correspondence to: Dipankar Ray, PhD, Department of Radiation Oncology, University of Michigan, Ann Arbor, Michigan 48109. dipray@umich.edu; or David G. Beer, PhD, Departments of Radiation Oncology and Surgery, University of Michigan, Ann Arbor, Michigan 48109. dgbeer@umich.edu.

Author contributions: Experimental design and study concept: D.R., D.F-T., D.J.N., D.G.B.; Development of methodology: D.R., P.R., D.F-T., D.G.B.; Provided patient sample material and clinical information: J.L, K.L., A.C.; Tissue microarray and histology: S.O., D.T., D.G.B.; Statistical analysis and data interpretation: D.R., H.J., D.J.N., D.G.B.; Technical and laboratory support: D.R., P.R., D.F-T., Z.W., H-W.Y., M.S.M., T.H.; Study supervision: D.R., D.G.B.; Manuscript preparation: D.R., D.J.N., T.S.L., D.G.B.

Supplementary Material

Note: To access the supplementary material accompanying this article, visit the online version of *Gastroenterology* at www.gastrojournal.org, and at https://doi.org/10.1053/j.gastro.2019.10.040.

Conflicts of interest

The authors disclose no conflicts.

RESULTS: Progression of BE to HGD or EAC associated with changes in expression of mRNAs that encoded mucins and promoted inflammation and activation of ATM and the DNA damage response. As tissues progressed from BE to HGD to EAC, they increased expression of mRNAs encoding isoform 1 of RNF128 (Iso1) and decreased expression of Iso2 of RNF128. RNF128 is an E3 ubiquitin ligase that targets p53 for degradation. Incubation of BE cells with interferon gamma caused them to increase expression of Iso1 and reduce expression of Iso2. Iso1 was heavily glycosylated with limited ubiquitin ligase activity for p53, resulting in p53 stabilization. Knockdown of Iso1 in BE and EAC cells led to degradation of the mutant form of p53 and reduced clonogenic survival. In contrast, Iso2 was a potent ligase that reduced levels of the mutant form of p53 in BE cells. In BE cells, Iso2 was hypoglycosylated and degraded, via ATM and GSK3B-mediated phosphorylation and activation of the BTRC-containing SCF ubiquitin ligase complex. Simvastatin, which degrades the mutant form of p53, also degraded RNF128 Iso1 protein in BE cells and slowed growth of EAC xenograft tumors in mice.

CONCLUSIONS: We found that isoform 2 of RNF128 is decreased in BE cells, resulting in increased levels of mutant p53, whereas isoform 1 of RNF128 is increased in BE cells, further promoting the stabilization of mutant p53.

Graphical Abstract

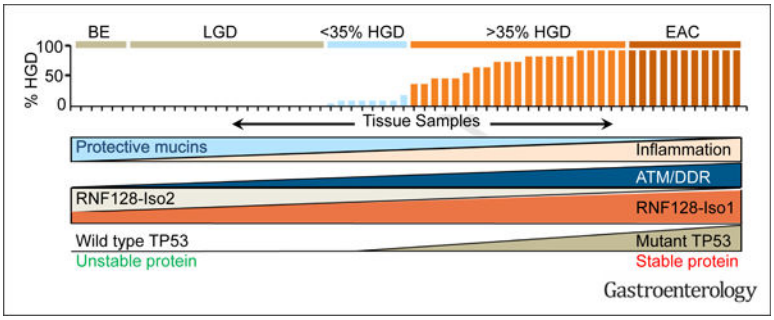

Keywords

Esophageal Cancer; Post-Transcriptional Regulation; Tumor Suppressor; Alternate Isoform

The presence of intestinal-type Barrett's metaplasia (BE), a condition in which the normal squamous mucosa is replaced by columnar epithelium, is associated with esophageal adenocarcinoma (EAC).[1,2] BE is increased in obese individuals, patients with acid reflux, and found in approximately 10% to 12% of these individuals at the time of initial endoscopy.[2] Patients with BE have an approximately 40-fold greater risk of EAC than the general population.[1] The malignant potential of this condition is evidenced by the progression of nondysplastic BE to low-grade dysplasia (LGD), high-grade dysplasia (HGD), and finally to invasive EAC. For this reason, patients with diagnosed BE are enrolled in regular endoscopic surveillance.

Our analysis of specific loci, comprehensive analyses of the specific DNA copy number changes,[3,4] and gene mutations associated with[5] and underlying EAC development[6] reveal substantial molecular heterogeneity of EAC, yet 70% to 80% of dysplastic BE and EAC contain *TP53* mutations (*TP53**).[5] In the present studies, we provide insight into the

molecular events that may put BE with dysplastic changes at increased risk for developing EAC. We show BE progression is associated with loss of mucin, increased ATM-DNA damage response, and increased splicing, which correlate with specific RNF128 isoform changes that occur concurrently with *TP53**. Importantly, these isoforms can form either homo- or heterodimers that dictate their ability to ubiquitinate TP53 and regulate its protein stability. RNF128 Iso2 (RNF128 isoform 202 [ENST00000324342])-specific protein degradation occurs via ATM/GSK3β-mediated phosphorylation followed by SCF$^{\beta\text{-TrCP1}}$-mediated proteasomal degradation, and the hyperglycosylated Iso1 (RNF128 isoform 201 [ENST00000255499]) appears to play a direct role in stabilizing the TP53* protein. Treatment with simvastatin reduced RNF128 Iso1 protein levels to impact the TP53 steady-state level, thus reduced colony formation in immortalized BE cells containing TP53* and further inhibited tumor growth, suggesting potential strategies for reducing cancer development in patients with BE.

Materials and Methods

ENSEMBL lists 2 observed isoforms for *RNF128*: ENST00000255499 (Iso1) encoding a 428aa protein, and ENST00000324342 (Iso2) which transcribes a 402aa protein. We used a rabbit polyclonal anti-RNF128 (Catalog no. ab137088; Abcam, Burlingame, CA) that recognizes both isoforms and an Iso1-specific sheep polyclonal antibody (Catalog no. AF6234; R&D Systems, Minneapolis, MN) to investigate RNF128 isoforms. Our attempted Iso2-specific antibody was nonspecific, as the region specific for Iso2 was nonantigenic (not shown). Other antibodies, cell culture details, and key reagents sourced for this study are listed in the Supplementary Methods.

Analysis of BE Progression Changes Using RNA Sequencing

Esophageal tissues were fresh frozen from individuals who underwent esophagostomy through the University of Michigan Health System between 1992 and 2015 using procedures approved by the institutional review board. Cryostat sectioning of Barrett's mucosa allowed the careful macrodissection of the epithelium before isolation of messenger RNA (mRNA) and DNA, as previously described.[7] Tissues from patients undergoing resection for HGD or EAC were histopathologically characterized[8] for the percentage of LGD or HGD in 10% increments. Sample mRNA with RNA integrity number scores >7.0 were used in paired-end sequence analysis of 120 million 100–base pair reads per lane using Illumina sequencers. Strand-specific RNA sequencing (RNAseq) libraries were prepared,[9] with read alignment performed using Bowtie (0.12.8) supplied with the set of annotated *Homo sapiens* transcript models (GENCODE v.17) containing 57,281 genes and 194,871 transcripts. Alignment of 3.7 billion strand-specific read pairs resulted in 2.5 billion (68%) that aligned uniquely (range: 26–51 million; median: 36 million). Gene and transcript expression level quantification was performed using rSeq (0.1.0) and defined as RPKM (reads per kilobase of exon model per million mapped reads) units. Statistical analysis was performed on log-transformed expression levels (log[RPKM+1]). Data analyses included 2 sample Welch's *t* test and Wilcoxon rank-sum tests between BE and LGD vs HGD and EAC, as well as between BE and LGD vs HGD (excluding EAC). Fold-change of expression levels between

BE and LGD vs HGD was summarized as the ratio of the average expression levels between the 2 groups. False discovery rates were computed using Storey's "q value" method.[10]

Immunohistochemistry and Automated Quantitative Immunofluorescence Analysis

The tissue microarray (TMA) contained BE tissues from 100 patients resected for HGD or EAC, including nondysplastic BE, LGD, and HGD, as well as normal esophageal squamous mucosa. Images of each core were microscopically captured at 3 extinction/emission wavelengths and distinguished from stroma and necrotic areas by epithelial cytokeratin staining. The RNF128 protein/antibody complex pixel intensities were machine-read, with cores not passing software quality-assurance checks excluded. Each patient's BE tissue RNF128 Iso1 staining in the TMAs was represented by 2 cores and results averaged. Statistical analysis between baseline characteristics of Iso1 staining in BE, LGD, and HGD groupings, as well as relationship of each isoform to level of TP53 protein, were carried out using linear regression with $P < .05$ deemed significant. The association between TP53 protein accumulation status and Iso1 expression was assessed using analysis of variance. Automated Quantitative Immunofluorescence Analysis (AQUA) was performed as described[11] to determine protein levels based on automated quantification of fluorescence.

Transfection and Protein Analyses

BE cells were transfected using Fugene HD reagent according to manufacturer's protocol. HEK-293 cells were transfected using calcium phosphate–mediated transfection, whereas HeLa cells were transfected with Lipofectamine 2000 according to the manufacturer's protocol. For small interfering RNA (siRNA), Lipofectamine RNAimax was used as described previously.[12] Immunoblot analysis and immunoprecipitation techniques were as described previously.[12]

Protein Half-Life Studies

RNF128 Iso1 and Iso2 protein half-lives in CpA and CpD cells were determined by adding cycloheximide (50 μg/mL) 24 hours after transfection, and cells were harvested at the indicated times posttreatment, then immunoblotted using antibodies to V5 (for RNF128) and GAPDH. The approximate RNF128 protein half-life ($t_{1/2}$) in CpA and CpD cells was calculated by plotting relative band density (arbitrary units) and time (hour) in a linear scale calculated from 3 independent experiments.

Coupled Transcription and Translation of RNF128 and In Vitro Ubiquitination

RNF128 Iso1 and Iso2 plasmids were subjected to cell-free protein expression using the TnT T7 quick coupled transcription/translation system according to manufacturer's protocol, with protein sizes confirmed by immunoblotting. The in vitro translated protein was then subjected to in vitro ubiquitination assay, as described previously.[13] For each reaction, 5 μL of RNF128 isoforms was used in the presence of 500 ng of recombinant wild-type TP53, with the TnT kit used for synthesis of $TP53^{R273H}$ protein. To set up in vitro ubiquitination, RNF128 proteins were used as E3 and TP53 proteins as substrates, reaction mixtures incubated for 10 minutes at 37°C, then reactions were stopped by adding 4X sample loading dye and subjected to immunoblotting using appropriate antibodies.

Immunofluorescence Studies

Immunofluorescence staining was performed as described previously[12] and fluorescent images were acquired using a DS-Fi1 (Nikon, Melville, NY) camera fitted on an Olympus (Tokyo, Japan) 1X-71 microscope.

Animal Studies

Animal experiments were performed according to University of Michigan–approved protocols and regulatory standards. Simvastatin was made in dimethyl sulfoxide. Athymic nude female mice (4–5 weeks old) (CB17SC-F; Taconic Biosciences, Albany, NY) bearing OE-33 flank tumors were dosed at 20 mg/kg via intraperitoneal injection every day for the first 2 weeks for efficacy studies. Control mice were treated with vehicle control. Tumor length and width were measured daily. Tumor volume was calculated as follows: volume (cm^3) = ($L \times W^2$)/2. Thirty days after tumor detection, mice were euthanized, and tumors were harvested. The effects of simvastatin on RNF128, TP53, acetylated TP53 (transcriptionally active) and GAPDH (loading control) were analyzed by immunoblotting.

Results

Identification of Transcriptional Changes During BE Progression

We used tw2o independent sample sets from patients undergoing esophagectomy for HGD or cancer using RNAseq (n = 65; dbGAP# in progress) and Affymetrix arrays (n = 46; GEO#GSE37203) to examine transcriptome expression during BE progression to EAC. Macro-dissected BE mucosa were used for mRNA isolation, and each histology percentage in 10% increments defined by pathologic review. They were organized (Figure 1A) from 100% nondysplastic BE to 100% HGD and >70% EAC cell-content, to compare mRNA changes from BE, LGD, and HGD to EAC. Our RNAseq BE progression cohort included 29 HGD samples, and genes and pathways associated with the high-risk HGD and EAC, relative to the lower-risk BE and LGD tissues were confirmed in Affymetrix arrays (Supplementary Figure 1A; Supplementary Tables 1 and 2).

Isoform-specific Changes in RNF128 (Grail) During BE Progression

Pathway enrichment for the most differential genes (Welch's *t* test $P < .05$ and mean-group fold change >2 or <0.5) during BE progression to EAC, assessed via DAVID,[14] revealed increased cell proliferation, with spliceosome machinery being more active in HGD and EAC, relative to BE (Supplementary Figure 1B; Supplementary Tables 3 and 4). Many spliceosome-related genes increasing from BE to EAC were confirmed in the Affymetrix cohort (Supplementary Figure 1B). Analysis revealed significantly increased transcript variance in HGD and EAC relative to BE and LGD samples (Supplementary Figure 1C). We examined potential gene-specific isoform changes during BE progression revealing multiple genes expressing multiple isoforms altered (Supplementary Table 5). Dramatic isoform-specific changes were observed for *RNF128* (Grail) during the transition of BE/LGD to HGD/EAC, with *Iso2* mRNA reduction in HGD and EAC relative to BE/LGD, coinciding with a trend for increased *Iso1* levels. Plotting the log2 ratio of both expressed isoforms demonstrates an "isoform switch" reflecting significant reduction of *Iso2* in HGD and EAC

(Figure 1B). As validation, we examined *RNF128* isoform expression in an independent cohort of 154 BE to HGD progression samples, as well as 122 EACs using quantitative reverse-transcription polymerase chain reaction. We observed a similar change in the log2 ratio of the 2 expressed isoforms in both cohorts, confirming the reduction of *Iso2* mRNA identified by RNAseq (Figure 1C).

Increased RNF128 Iso1 Protein Expression Is Associated With TP53 Protein Accumulation and TP53 Mutation

RNF128 is an E3-ubiquitin ligase causing T-cell anergy[15]; however, one report[16] indicates it functionally interacts with the N-terminus of TP53 to target its degradation and modulating TP53 transactivation activity under stress conditions. RNF128 has mutually exclusive first exons resulting in 2 isoforms conserved throughout jawed vertebrates,[17] yet with no published isoform functional comparisons. Commercial antibodies detecting both RNF128 isoforms (Abcam, Cambridge, MA) and an Iso1-specific antibody (R&D Systems, Minneapolis, MN) were used to assess protein levels in BE-HGD samples via TMA. Using AQUA,[11] we determined concomitant protein levels based on automated quantification of fluorescence for both Iso1 and TP53 along with cell nuclei stained with 4′,6-diamidino-2-phenylindole. Iso1 was significantly increased in HGD and EAC relative to BE/LGD, and highly correlated to nuclear accumulation of TP53 ($r = 0.69$; Figure 1D), and often indicative of *TP53** mutation.[18] Pixel-based colocalization across the BE cohort using Fiji software confirmed this association nonparametrically (rho = 0.86; Supplementary Figure 2). When *TP53** status was considered in 181 available BE samples (both RNAseq and validation cohorts), alongside 2 previously published EAC cohorts we observed approximately 70% of HGD and EAC samples contained *TP53* mutations and significantly less frequent in the nondysplastic BE (19%) or LGD (33%) samples (Supplementary Table 6).

Protein ubiquitination is critical for maintaining protein stability, localization, and function, including TP53.[19,20] Ubiquitination is a multistep process regulated by 3 enzyme categories, known as E1, E2, and E3. E1 (ubiquitin-activating enzyme) is common to most reactions in a cell, whereas, E2 (ubiquitin-conjugating enzyme) and E3 (ubiquitin ligase) family members have distinct substrate specificities. Wild-type TP53 protein is very labile and a growing list (>10) of E3s can control TP53 protein stability and function.[19] Among these, RING E3 family member MDM2 is well-studied, whereas RNF128 is a relatively new inclusion. Based on literature and our preliminary data, we hypothesize significant similarities between MDM2 and RNF128 modes of action. Analysis of our RNAseq data for reported E3s, *RNF128* isotype switching was observed, whereas other E3 mRNAs showed minimal changes in BE progression (Supplementary Table 7). On average, *MDM2* expression (RNAseq) was 3.2 times lower than *RNF128* across BE samples (Supplementary Figure 3A) and *MDM4* to *MDM2* levels are unchanged during BE progression. RNAseq-based expression of RNF128 Iso1 and Iso2, as well as MDM2, in BE progression (BE and LGD compared with HGD; Supplementary Figure 3C), and TCGA EAC cohorts (ref) (Supplementary Figure 3D) showed a 5% minority of HGD (1/20) and EAC (4/89) samples with very high MDM2 expression, for which MDM2 may be an important driver. Overall RNF128 appears to be a critical E3 ubiquitin ligase in the regulation of TP53 protein

stability during BE progression to EAC. Interestingly, tissues of endodermal origin show the highest *RNF128* expression, a pattern not seen for *MDM2* (Supplementary Figure 3B).

Loss of Protective Mucins and Activation of the DNA Damage Response Associates With RNF128 Isoform Switching

We hypothesized that increased spliceosome activity during BE progression reflects DNA damage and resulting ATM-dependent signaling in dysplastic BE cells. Mucin gene expression (*MUC5AC, 3A, 17*) is dramatically decreased in both RNAseq and Affymetrix cohorts (Figure 2A; Supplementary Table 8), consistent with loss of goblet cells in LGD and HGD seen in histopathologic preparations stained with hematoxylin-eosin (Figure 2A) and previous studies of BE and EAC.[21,22] Many goblet cell–related genes are reduced during BE progression (Figure 2B). To assess protein-related changes in DNA damage and ATM kinase signaling, we examined our TMA using antibodies to phospho-H2AX (γH2AX) and its association with mucin and ATM. Mucin stains (Alcian blue–periodic acid Schiff reagent) show nondysplastic BE retains abundant blue goblet cells that are lost in dysplastic BE (Figure 3A). Concurrent with mucin loss, which functionally protects BE cells against acid/bile reflux–induced cellular damage, we observe increased expression of "DNA damage response" genes, including *ATM, MRE11, P53BP1,* and *RAD50* (Figures 2A, and 3B and C; Supplementary Figure 4). Consistent with a previous study,[23] we found γH2AX staining was increased in dysplastic BE cells but not nondysplastic glands retaining goblet cells (Figure 3A). Phospho-ATM staining was higher in dysplastic BE cells (Figure 3A). Thus, loss of protective mucins in dysplastic BE may lead to DNA damage and initiate phosphorylation of H2AX by the ATM kinase. As recently reported, the core spliceosome is a target and effector of noncanonical ATM signaling.[24]

Interferon Signaling Modulates RNF128 Isoform Expression

The stimuli for the reduction of *Iso2* in HGD and EAC may reflect increased inflammation during BE progression or acid- or oxidative product–induced DNA damage. Interferon (IFN)γ is a master regulator of cytokine signaling.[25] We observed many interferon-inducible transcripts, including *PTGS2* (Cox2) and *LCN2* increase in HGD and EAC (Figure 3D) and IFNγ treatment (10 ng/mL) altered the isoform ratio in BE cells (CpA; wild-type TP53 and CpD; TP53*c.904delC) (Figure 3E) as seen in HGD and EAC (Figure 1B). A similar response was observed in EAC (OE19; TP53*c.929–930ins1 and OE33; TP53*c.404G>A) cells (not shown).

RNF128 Iso1 Stabilizes, but Iso2 Degrades TP53*

As RNF128 is a reported E3 ligase for TP53,[16] we examined the effect of either knockdown or overexpression of Iso1 and Iso2 on TP53 and TP53* protein levels in CpA and CpD cells, respectively. Using 2 different siRNAs, Iso1 knockdown caused TP53* loss in CpD cells with concomitant reduction in clonogenic survival (Figure 4B). Loss of Iso2 had no major impact both on TP53* and clonogenic survival in CpD cells, whereas Iso2 knockdown in CpA cells resulted in TP53 accumulation and loss of clonogenic survival (Figure 4C and D). At the transcript level, knockdown of one isoform caused compensatory upregulation of the other (Supplementary Figure 5A and B), also seen at the protein level using Iso1-specific antibody (Figure 4C). To confirm the CpD cell's clonogenic survival dependency on TP53*,

we performed siRNA-mediated TP53 knockdown. As shown in Figure 4E and F, TP53 loss had no impact on CpA cells; however, TP53* knockdown in CpD cells reduced clonogenic potential 50%, suggesting TP53* addiction. Overexpressing Iso2 in CpD cells reduced levels of endogenous TP53*, whereas Iso1 overexpression resulted in an approximately 30% increase in TP53* (Figure 4G). Similar observations were noted following cotransfection of Iso1 and $TP53^{R273H}$ mutant in HEK-293 cells (Figure 4H). In CpA, we tested the effect of Iso1 overexpression on endogenous wild-type TP53, and in the presence of individually transfected TP53*, including C135S, R175H, R213Q, and R248Q mutations. As shown in Figure 4I, TP53* steady-state levels were increased in all cases. Alterations of RNF128 Iso1 and Iso2 levels, either via knockdown or overexpression, had minimal impacts on *TP53*/*TP53** transcript levels (Supplementary Figure 5A–C). Protein half-life studies using the protein synthesis inhibitor cycloheximide, showed increased TP53* (R175H) protein stability in the presence of Iso1 (Figure 4J and K), suggesting its protective role on TP53*. Similar differences were obtained in other mutants (not shown). Interestingly, in these experiments, once Iso1 levels started to decrease (relatively shorter half-life compared with TP53*), TP53* levels were reduced. These data support our clinical observation that increased RNF128 Iso1 expression is associated with TP53* stability during BE progression.

To understand the differential impact of Iso1 and Iso2 on TP53*, we performed ubiquitination assays both *in cells* and *cell-free* conditions. Iso2 overexpression resulted in polyubiquitination-mediated degradation of $TP53^{R273H}$, inhibited using proteasomal inhibitor MG132 (Figure 5A). In contrast, Iso1 overexpression reduced the abundance of TP53* (DDK-tagged $TP53^{R248Q}$) polyubiquitinated species relative to basal polyubiquitination levels, suggesting an Iso1 protective effect on TP53* polyubiquitination (Figure 5B). Using *cell-free* ubiquitination assays, Iso2 efficiently polyubiquitinated both wild-type and $TP53^{R273H}$, whereas Iso1 had limited TP53 polyubiquitination ability (Figure 5C). Using various mutant ubiquitin molecules (ie, K11R, K48R, and K63R), we noted differences in Iso2-mediated polyubiquitination linkage on wild-type and $TP53^{R273H}$. Importantly, in both assays (Figure 5B and C), Iso1 showed a dominant negative effect on Iso2-mediated TP53/TP53* polyubiquitination.

Homo- and/or Heterodimerization Affects RNF128 Ubiquitin Ligase Activity to Regulate TP53 Stability

As TP53-targeting E3s, including MDM2 and MDM4, form homo- or heterodimers for their activity, and unpublished crystal data of the N-terminal domain (PDB#3icu) suggest RNF128 may form a dimer, we tested the dimerization potential of RNF128 isoforms. Using disuccinimidyl suberate (DSS), a protein cross-linking agent, Iso1 and Iso2 showed differential dimerization potential; although a DDK-tagged Iso1 formed homodimers effectively, similarly tagged Iso2 homodimers did not (Figure 5D) and Iso1 and Iso2 heterodimers were most prevalent. These data were confirmed by overexpressing DDK-tagged Iso1 and V5-tagged Iso2 proteins in the presence and absence of DSS followed by immunoprecipitation and immunoblotting (Supplementary Figure 6B), showing Iso1-Iso2 heterodimers are preferred. Detection of oligomers was more robust with anti-DDK than anti-V5 for unknown reasons (Supplementary Figure 6A). Together, RNF128 isoforms may

act similarly to MDM2/MDM4, where MDM2 and MDM4 can form homo/heterodimers, yet only MDM2 has intrinsic ubiquitin ligase activity.[26,27] MDM2 homo- and MDM2-MDM4 heterodimers play a critical role in determining TP53 protein stability in certain tissues.[28–31] To assess the impact of Iso1 and Iso2 on regulating TP53* protein stability, we cotransfected DDK-tagged $TP53^{R248Q}$ in the presence of either Iso1 or Iso2 tagged with V5, or in combination. As shown in Figure 5E, Iso2-induced TP53* downregulation was partially compromised with Iso1. Similarly, using a *cell-free* ubiquitination assay, Iso1 addition inhibited Iso2-mediated TP53/TP53* polyubiquitination (Figure 5C), implicating a negative regulatory function of RNF128 heterodimers.

Iso2 Is a Relatively Unstable Protein Compared With Iso1 and a Novel Substrate of β-TrCP1

In BE (CpA and CpD), HeLa, and HEK-293 cells, Iso2 steady-state levels were consistently lower compared with Iso1 (Figure 4G). Because Iso1 and Iso2 complementary DNA expression constructs used a cytomegalovirus-driven promoter, possible differential transcription rates were ruled out using reverse-transcription polymerase chain reaction (Supplementary Figure 5C). To assess altered protein stability on differential expression, we performed protein half-life studies using cycloheximide. As shown in Figure 6A and C, and quantified in Figure 6B and D, Iso2 has a shorter half-life (54 and 40 minutes in CpA and CpD cells, respectively) compared with Iso1 (100 and 120 minutes in CpA and CpD, respectively). Analysis of RNF128 amino acid sequence, revealed a consensus phospho-degron ($D^{p}SGxx^{p}S$, where ‘x’ could be any amino acid[32]) in the C-terminal end of both RNF128 isoforms (363-SSGYAS-368), which when phosphorylated may be recognized and degraded by t F-box family ubiquitin ligase β-TrCP (Figure 6E, top). Overexpression of β-TrCP1, but not β-TrCP2, efficiently downregulated RNF128 and a dominant negative β-TrCP1 increased steady-state level (Figure 6E, bottom). Conversely, siRNA-mediated β-TrCP1 knockdown increased RNF128 levels (Supplementary Figure 7A). To define the role of serine (S) phosphorylation, we mutated S to alanine (A) (SA), which significantly stabilized the Iso2 protein and also affected Iso1 levels slightly (Figure 6F). Using immune pull-down assays, the SA mutant interacted less efficiently with β-TrCP1, suggesting a critical role of this serine residue in maintaining RNF128 protein stability (Figure 6G). As inflammation and DNA damage are associated with RNF128 isoform switching, we focused on kinase(s) modulated by such insults, particularly ATM, GSK-3β, and casein kinase I, using specific inhibitors. Both ATM and GSK-3β inhibitors effectively inhibited β-TrCP1-mediated RNF128 downregulation (Supplementary Figure 7B). For confirmation, we used GSK-3β–specific siRNAs, which showed similar rescue (Supplementary Figure 7C). Thus, RNF128 (particularly Iso2) is a novel substrate for $SCF^{\beta\text{-TrCP1}}$, with environmental stimuli undergoing ATM/GSK-mediated phosphorylation to be recognized and degraded by β-TrCP1. Such posttranslational protein regulation and splicing/promoter switching might reduce Iso2 expression, and change Iso1:- Iso2 ratio balance toward Iso1 homo-dimerization, thus reducing polyubiquitination and stabilizing TP53* protein.

Glycan moiety attachment can modulate a protein’s stability.[33] N-linked glycosylation also affects protein dimerization.[34] As RNF128 is a glycosylated protein,[16] and we demonstrated RNF128 isoform-specific differential protein stability, we examined glycosylation’s impact on isoform-specific homo-/heterodimerization and protein stability. Iso1 (428 aa) and Iso2

(402 aa) are predicted as 47 and 45 kDa respectively, yet the observed molecular weights were >65 kDa (Figure 4G, Supplementary Figure 8A), suggesting posttranslational modification, differentially impacted by the presence of wild-type and TP53*. There are 5 and 3 unique (N-terminal), and 2 common (C-terminal) probable glycosylation sites in Iso1 and Iso2, respectively (Supplementary Figure 8A), confirmed in CpA cells overexpressing RNF128 Iso1 using tunicamycin (Supplementary Figure 9A), and consistent with previous observations.[16] We noted reduced RNF128 Iso1 steady-state levels on tunicamycin treatment (Supplementary Figure 9B), and reduced Iso1 homodimerization (Supplementary Figure 9B). We expressed either wild-type or SA mutants of DDK-tagged Iso2 in the presence or absence of V5-tagged Iso1. Iso1 promoted heteromerization with Iso2, which further increased Iso2 steady-state levels, and was impacted by phosphorylation (Supplementary Figure 9C). We propose a model (Supplementary Figure 9D) wherein BE, Iso1, and Iso2 exist in a dynamic balance, whereby homo- and heterodimers have differing levels of protein stability and ubiquitin ligase activity. Localization studies of Iso1 (Supplementary Figure 8B and C; video link) showed a perinuclear punctate pattern, colocalizing with the early endosomal marker (EEA1) (Supplementary Figure 8B), suggesting Iso1 resides in endosomes.

Simvastatin Efficiently Downregulates Iso1 and TP53* to Control Tumor Growth

Simvastatin can exert pleotropic effects via multiple mechanisms; particularly, statin negatively impacts TP53* protein levels via inhibition of mevalonate pathway and recruitment of a U-family ubiquitin ligase.[35,36] Also, statin has shown to cause degradation of an F-box family E3, SKP2 to cause P21 and P27 protein accumulation.[37] While examining simvastatin effects on the clonogenic survival of immortalized BE cells, we noted TP53*-driven CpD cells are more sensitive to simvastatin relative to wild-type TP53 containing CpA cells (Figure 7A). This correlated with reduction in both RNF128 Iso1 and TP53* levels in simvastatin-treated CpD cells (Supplementary Figure 10A). Interestingly, siRNA-mediated Iso1 knockdown further sensitized CpD cells to simvastatin (Figure 7A), whereas Iso2 loss reduced simvastatin potency in TP53*-driven CpD and EAC cells (not shown).

To test the in vivo efficacy of simvastatin in preclinical models, we examined the tumor-forming potential of BE cells in nude mice. Immortalized CpA and CpD cells are not transformed, and injection of 5 million cells failed to form tumors even using matrigel (not shown). The OE33 EAC cell line was then selected for tumor xenograft studies. siRNA-mediated TP53* knockdown in OE33 cells resulted in 60% reduction in clonogenic survival, suggesting TP53* dependency (Figure 7B). Athymic nude female mice were injected subcutaneously with OE33 cells on both the flanks and randomized into 2 groups, then at day 7 post-detection of palpable tumors (tumor size 50–100 mm^3), half (n = 8 flank tumors in 4 mice) were injected (intraperitoneally) with simvastatin, which blocked tumor growth for an observation period of 30 days, whereas vehicle-treated tumors continued to grow (n = 7 flanks in 4 mice: 1 OE33 flank injection did not produce a tumor (Figure 7C). We noted a robust difference ($P = .00017$, Wilcoxon rank-sum test) in relative change in tumor volumes between day 7 and 21 post tumor detection between vehicle and simvastatin-treated groups (Figure 7D) correlating with reduced proliferation (Supplementary Figure 10C), and reduced

levels of Iso1 and TP53* (Figure 7E and F). In cell lines, simvastatin-induced Iso1 and TP53* downregulation was inhibited by proteasomal inhibitor MG132 (Supplementary Figure 10A and B). These data suggest Iso1 levels help maintain TP53* and that agents that reduce Iso1 protein levels promote TP53* loss and inhibit tumor growth, at least for a subset of TP53*-dependent models. Although statin is can elicit an anti-IFNγ response in many instances, while analyzing simvastatin effects on rescuing IFNγ-mediated RNF128 transcript isoform switch, we noted minimal transcript rescue potential (Supplementary Figure 10D). In contrast, our data consistently indicate statin can downregulate RNF128 Iso1 protein, which in turn may be causing TP53* destabilization in this model. To graphically summarize our findings, we propose a model (Supplementary Figure 11) incorporating our results and RNF128 isoform switching, to explain the increased TP53* stability during BE progression.

Discussion

TP53 gene mutations are the most frequent genetic alteration in EAC[5], occurring in >70% of cancers and often arise late in BE progression, with *TP53** cells undergoing genome doubling and subsequent oncogenic amplifications. Our observed frequency of *TP53** in HGD is comparable to EAC (Supplementary Table 6), indicating the critical role of TP53* in BE progression and known higher risk of progression to EAC among patients diagnosed with HGD.[1] Using RNAseq, we examined isoform-specific transcriptional events associated with BE progression, emphasizing the less characterized HGD mucosa. Pathways affected during BE progression, including increased cell proliferation and decreased differentiation, have been previously observed[38]; however, increased spliceosome activity, altered IFNγ signaling, and pronounced *RNF128* isoform changes were seen, with significant reduction of *Iso2* mRNA in HGD and EAC relative to BE (Figure 1B). Other genes also showed dramatic isoform changes in HGD and EAC (Supplementary Table 5), potentially correlating with the increased splicing and/or promoter utilization as a consequence of the oxidative damage associated with loss of protective mucins and activation of ATM and the DNA damage response (Figures 2 and 3). The core spliceosome machinery is a reported target and effector of noncanonical ATM signaling,[24] and we observed increased ATM/pATM expression in areas of HGD showing increased γH2AX (Figure 3A); however, we have not explored the link between RNF128 isoform changes and ATM signaling in BE progression. RNF128 Iso1 protein analysis showed increased expression in HGD concordant with TP53 nuclear protein accumulation (Figure 1D and Figure 5). Importantly, overexpression of Iso2 reduced the steady-state levels of TP53* (Figure 5).

Iso1 and Iso2 have differential impacts on TP53. Using *cell-free* ubiquitination assays, Iso2 overexpression increased, whereas Iso1 inhibited Iso2-mediated $TP53^{R273H}$ polyubiquitination (Figure 5C). Similarly, in cells, Iso2 efficiently polyubiquitinated $TP53^{R248Q}$ mutant, whereas Iso1 had minimal TP53 polyubiquitinating ability and Iso1 significantly inhibited Iso2-mediated TP53 polyubiquitination (Figure 5B). Importantly, in BE cells, overexpression in the presence and absence of protein cross-linking (DSS treatment) followed by immunoblotting, Iso1 was found to form homodimers; however, Iso1-Iso2 heterodimers are preferred (Figure 5D). RNF128 isoform interactions appear similar to MDM2 and MDM4, with regard to TP53 degradation, where heterodimers are

preferred yet MDM2 alone has intrinsic ubiquitin ligase activity.[28] *MDM2* and *MDM4* expression is unchanged in BE progression, and both showed very low expression relative to *RNF128* (Supplementary Figure 3), supporting RNF128 as the critical ubiquitin ligase for TP53 in BE cells.

RNF128 is a glycosylated protein,[16] and we observed isoform-specific glycosylation that alter homo-/heterodimerization of RNF128, its ubiquitin ligase activity, and cellular localization. Glycosylation was differentially impacted by wild-type and TP53*; Iso1 is hyper-modified in the presence of TP53*, whereas Iso2 was hypo-modified (Figure 4G and H). Green fluorescent protein–tagged (live cell imaging) or DDK-tagged (immunofluorescence staining) RNF128 constructs showed perinuclear and endosomal punctate localization (Supplementary Figure 8B and C; video link). Tunicamycin treatment reduced Iso1 and altered its cellular localization, suggesting glycosylation may be critical for maintaining its localization and protein stability. We show Iso2 is relatively unstable, with a much shorter half-life relative to Iso1 (Figure 6A–D), and importantly is a novel β-TrCP1 substrate (Figure 6E–G). We identified a consensus phospho-degron ($D^{p}SGxx^{p}S$) in the C-terminal end of both the RNF128 isoforms (SSGYAS), which when phosphorylated may be recognized and degraded by the F-box family ubiquitin ligase β-TrCP1, but not β-TrCP2 (Figure 6E–G). ATM and GSK-3β inhibitors prevented β-TrCP1-mediated RNF128 downregulation, connecting their roles in inflammation and DNA damage response with RNF128 isoform switching.

A meta-analysis of 13 clinical trials revealed that patients with preexisting Barrett's mucosa prescribed statins showed a 30% reduction in EAC incidence.[39] The exact mechanism underlying this substantial cancer reduction is unknown, and likely reflects pleotropic effects. Prominently, statin inhibits the mevalonate pathway, impairing TP53* interaction with DNAJA1 (an HSP40 family member) and instead promotes CHIP (a U-box family ubiquitin ligase)-mediated degradation.[35] In hepatocellular carcinoma, statin downregulates SKP2, an F-box family ubiquitin ligase causing accumulation of growth inhibitory P21 and P27 proteins. There are instances where anticancer ability may relate to statin's anti-inflammatory activity, and reported IFNγ signaling inhibition.[40] Cox2 plays an established role in BE progression,[41] and IFNγ-induced Cox2 is inhibited with simvastatin.[42] Using clonogenic survival assays, we noted that CpD BE cells containing TP53* are slightly more sensitive to simvastatin (half maximal inhibitory concentration [IC_{50}] 40 nM) relative to wild-type TP53 containing CpA cells (IC_{50} 95 nM), and Iso1 loss further sensitized CpD cells (IC_{50} ~6 nM). In addition, in vivo treatment with simvastatin blocked tumor xenograft growth of TP53*-driven EAC (OE33) cells (Figure 7). Tumors from simvastatin-treated mice showed reduction in Iso1 and loss of TP53*, compared with vehicle controls (Figure 7C and D). In contrast, within our experimental conditions, the potential of statin to restore IFNγ-mediated alteration of RNF128 isoform ratio, was marginal (Supplementary Figure 10D). Thus, RNF128 Iso1 levels may help maintain TP53* levels, and agents, such as statins, can reduce Iso1 protein levels causing TP53* loss and inhibition of oncogene-driven EAC cells. Future studies will define the importance of mevalonate pathway in statin-mediated downregulation of RNF128 Iso1 and role in TP53* degradation. As our data indicate that glycosylation plays an important role in RNF128 protein stability, and as statin is known to inhibit N-linked glycosylation of proteins,[43] it is plausible that statin-mediated

downregulation of RNF128 Iso1 may be due to the inhibition of glycosylation. We provide a model for the regulation of RNF128 based on our data (Supplementary Figure 11), which may provide a potential basis for strategies to reduce the incidence of TP53*-driven EAC in patients with BE.

Supplementary Material

Refer to Web version on PubMed Central for supplementary material.

Acknowledgments

We thank Dr Mats Ljungman for critical review of the manuscript, Daniel Zhou for technical assistance, and Steven Kronenberg for graphic assistance. We thank Drs Amitabh Chak (Department of Medicine, Case Western Reserve University) and Alexander Miron (AgriPlex Genomics) for providing *TP53* mutation typing in BE samples, which will be the subject of a separate manuscript. We also thank other members of the Ray and Beer laboratory for helpful discussion.

Funding

Research reported in this publication is supported by National Cancer Institute grants RO1CA215596, U54CA163059, P30CA046592, and F31A200113, and the John and Carla Klein Family research fund.

Abbreviations used in this paper:

BE	Barrett's esophagus
DSS	disuccinimidyl suberate
EAC	esophageal adenocarcinoma
HGD	high-grade dysplasia
IC_{50}	half maximal inhibitory concentration
IFN	interferon
Iso1	RNF128 isoform 201 (ENST00000255499)
Iso2	RNF128 isoform 202 (ENST00000324342)
LGD	low-grade dysplasia
mRNA	messenger RNA
RNAseq	RNA sequencing
siRNA	small interfering RNA
TMA	tissue microarray
TP53	wild-type TP53
TP53*	mutant TP53

References

1. Bresalier RS. Barrett's esophagus and esophageal adenocarcinoma. Annu Rev Med 2009;60:221–231. [PubMed: 18783330]
2. Shaheen NJ, Richter JE. Barrett's oesophagus. Lancet 2009;373:850–861. [PubMed: 19269522]
3. Dulak AM, Schumacher SE, van Lieshout J, et al. Gastrointestinal adenocarcinomas of the esophagus, stomach, and colon exhibit distinct patterns of genome instability and oncogenesis. Cancer Res 2012;72:4383–4393. [PubMed: 22751462]
4. Lin L, Bass AJ, Lockwood WW, et al. Activation of GATA binding protein 6 (GATA6) sustains oncogenic lineage-survival in esophageal adenocarcinoma. Proc Natl Acad Sci U S A 2012;109:4251–4256. [PubMed: 22375031]
5. Dulak AM, Stojanov P, Peng S, et al. Exome and whole-genome sequencing of esophageal adenocarcinoma identifies recurrent driver events and mutational complexity. Nat Genet 2013;45:478–486. [PubMed: 23525077]
6. Stachler MD, Taylor-Weiner A, Peng S, et al. Paired exome analysis of Barrett's esophagus and adenocarcinoma. Nat Genet 2015;47:1047–1055. [PubMed: 26192918]
7. Miller CT, Moy JR, Lin L, et al. Gene amplification in esophageal adenocarcinomas and Barrett's with high-grade dysplasia. Clin Cancer Res 2003;9:4819–4825. [PubMed: 14581353]
8. Skacel M, Petras RE, Gramlich TL, et al. The diagnosis of low-grade dysplasia in Barrett's esophagus and its implications for disease progression. Am J Gastroenterol 2000;95:3383–3387. [PubMed: 11151865]
9. Levin JZ, Yassour M, Adiconis X, et al. Comprehensive comparative analysis of strand-specific RNA sequencing methods. Nat Methods 2010;7:709–715. [PubMed: 20711195]
10. Storey JD, Dai JY, Leek JT. The optimal discovery procedure for large-scale significance testing, with applications to comparative microarray experiments. Biostatistics 2007;8:414–432. [PubMed: 16928955]
11. Camp RL, Dolled-Filhart M, King BL, et al. Quantitative analysis of breast cancer tissue microarrays shows that both high and normal levels of HER2 expression are associated with poor outcome. Cancer Res 2003; 63:1445–1448. [PubMed: 12670887]
12. Ray D, Ahsan A, Helman A, et al. Regulation of EGFR protein stability by the HECT-type ubiquitin ligase SMURF2. Neoplasia 2011;13:570–578. [PubMed: 21750651]
13. Shukla S, Allam US, Ahsan A, et al. KRAS protein stability is regulated through SMURF2: UBCH5 complex-mediated beta-TrCP1 degradation. Neoplasia 2014; 16:115–128. [PubMed: 24709419]
14. Huang DW, Sherman BT, Tan Q, et al. The DAVID Gene Functional Classification Tool: a novel biological module-centric algorithm to functionally analyze large gene lists. Genome Biol 2007;8:R183. [PubMed: 17784955]
15. Anandasabapathy N, Ford GS, Bloom D, et al. GRAIL: an E3 ubiquitin ligase that inhibits cytokine gene transcription is expressed in anergic CD4+ T cells. Immunity 2003;18:535–547. [PubMed: 12705856]
16. Chen YC, Chan JY, Chiu YL, et al. Grail as a molecular determinant for the functions of the tumor suppressor p53 in tumorigenesis. Cell Death Differ 2013;20:732–743. [PubMed: 23370271]
17. Abascal F, Tress ML, Valencia A. The evolutionary fate of alternatively spliced homologous exons after gene duplication. Genome Biol Evol 2015;7:1392–1403. [PubMed: 25931610]
18. Rodrigues NR, Rowan A, Smith ME, et al. p53 mutations in colorectal cancer. Proc Natl Acad Sci U S A 1990; 87:7555–7559. [PubMed: 1699228]
19. Hock AK, Vousden KH. The role of ubiquitin modification in the regulation of p53. Biochim Biophys Acta 2014; 1843:137–149. [PubMed: 23742843]
20. Jain AK, Barton MC. Making sense of ubiquitin ligases that regulate p53. Cancer Biol Ther 2010;10:665–672. [PubMed: 20930521]
21. Arul GS, Moorghen M, Myerscough N, et al. Mucin gene expression in Barrett's oesophagus: an in situ hybridisation and immunohistochemical study. Gut 2000; 47:753–761. [PubMed: 11076872]

22. Glickman JN, Blount PL, Sanchez CA, et al. Mucin core polypeptide expression in the progression of neoplasia in Barrett's esophagus. Hum Pathol 2006;37:1304–1315. [PubMed: 16949933]
23. von Holzen U, Chen T, Boquoi A, et al. Evidence for DNA damage checkpoint activation in barrett esophagus. Transl Oncol 2010;3:33–42. [PubMed: 20165693]
24. Tresini M, Warmerdam DO, Kolovos P, et al. The core spliceosome as target and effector of non-canonical ATM signalling. Nature 2015;523:53–58. [PubMed: 26106861]
25. Zha Z, Bucher F, Nejatfard A, et al. Interferon-gamma is a master checkpoint regulator of cytokine-induced differentiation. Proc Natl Acad Sci U S A 2017;114:E6867–E6874. [PubMed: 28760993]
26. Kostic M, Matt T, Martinez-Yamout MA, et al. Solution structure of the Hdm2 C2H2C4 RING, a domain critical for ubiquitination of p53. J Mol Biol 2006;363:433–450. [PubMed: 16965791]
27. Linke K, Mace PD, Smith CA, et al. Structure of the MDM2/MDMX RING domain heterodimer reveals dimerization is required for their ubiquitylation in trans. Cell Death Differ 2008;15:841–848. [PubMed: 18219319]
28. Iyappan S, Wollscheid HP, Rojas-Fernandez A, et al. Turning the RING domain protein MdmX into an active ubiquitin-protein ligase. J Biol Chem 2010;285:33065–33072. [PubMed: 20705607]
29. Plechanovova A, Jaffray EG, Tatham MH, et al. Structure of a RING E3 ligase and ubiquitin-loaded E2 primed for catalysis. Nature 2012;489:115–120. [PubMed: 22842904]
30. Poyurovsky MV, Priest C, Kentsis A, et al. The Mdm2 RING domain C-terminus is required for supramolecular assembly and ubiquitin ligase activity. EMBO J 2007; 26:90–101. [PubMed: 17170710]
31. Uldrijan S, Pannekoek WJ, Vousden KH. An essential function of the extreme C-terminus of MDM2 can be provided by MDMX. EMBO J 2007;26:102–112. [PubMed: 17159902]
32. Frescas D, Pagano M. Deregulated proteolysis by the F-box proteins SKP2 and beta-TrCP: tipping the scales of cancer. Nat Rev Cancer 2008;8:438–449. [PubMed: 18500245]
33. Sola RJ, Rodriguez-Martinez JA, Griebenow K. Modulation of protein biophysical properties by chemical glycosylation: biochemical insights and biomedical implications. Cell Mol Life Sci 2007;64:2133–2152. [PubMed: 17558468]
34. Zhuo Y, Yang JY, Moremen KW, et al. Glycosylation alters dimerization properties of a cell-surface signaling protein, carcinoembryonic antigen-related cell adhesion molecule 1 (CEACAM1). J Biol Chem 2016;291:20085–20095. [PubMed: 27471271]
35. Parrales A, Ranjan A, Iyer SV, et al. DNAJA1 controls the fate of misfolded mutant p53 through the mevalonate pathway. Nat Cell Biol 2016;18:1233–1243. [PubMed: 27775703]
36. Parrales A, Thoenen E, Iwakuma T. The interplay between mutant p53 and the mevalonate pathway. Cell Death Differ 2018;25:460–470. [PubMed: 29238070]
37. Wang X, Zhai H, Wang F. 6-OHDA induces oxidation of F-box protein Fbw7beta by chaperone-mediated autophagy in Parkinson's model. Mol Neurobiol 2018; 55:4825–4833. [PubMed: 28733899]
38. Varghese S, Newton R, Ross-Innes CS, et al. Analysis of dysplasia in patients with Barrett's esophagus based on expression pattern of 90 genes. Gastroenterology 2015; 149:1511–1518.e5. [PubMed: 26248086]
39. Singh S, Singh AG, Singh PP, et al. Statins are associated with reduced risk of esophageal cancer, particularly in patients with Barrett's esophagus: a systematic review and meta-analysis. Clin Gastroenterol Hepatol 2013; 11:620–629. [PubMed: 23357487]
40. Jain MK, Ridker PM. Anti-inflammatory effects of statins: clinical evidence and basic mechanisms. Nat Rev Drug Discov 2005;4:977–987. [PubMed: 16341063]
41. Morris CD, Armstrong GR, Bigley G, et al. Cyclo-oxygenase-2 expression in the Barrett's metaplasia-dysplasia-adenocarcinoma sequence. Am J Gastroenterol 2001;96:990–996. [PubMed: 11316217]
42. Lee CS, Shin YJ, Won C, et al. Simvastatin acts as an inhibitor of interferon gamma-induced cycloxygenase-2 expression in human THP-1 cells, but not in murine RAW264.7 cells. Biocell 2009;33:107–114. [PubMed: 19886038]

43. Forbes K, Shah VK, Siddals K, et al. Statins inhibit insulin-like growth factor action in first trimester placenta by altering insulin-like growth factor 1 receptor glycosylation. Mol Hum Reprod 2015;21:105–114. [PubMed: 25304981]

WHAT YOU NEED TO KNOW

BACKGROUND AND CONTEXT

Progression of Barrett's esophagus (BE) to dysplasia and esophageal adenocarcinoma (EAC) involves mutations in *TP53* that increase the stability of its product, p53. We analyzed BE tissues for transcripts that associate with BE progression and identified RNF128 that affects the stabilization of p53.

NEW FINDINGS

We found that reduced isoform 2 of RNF128, an E3 ubiquitin ligase, promotes stabilization of mutant forms of p53 found in BE cells. In addition, we show that increased isoform 1 levels also result in increased levels of p53 in BE cells.

LIMITATIONS

This study was performed in cell lines and mice.

IMPACT

We discovered a process by which a mutant form of a protein that promotes carcinogenesis is stabilized in BE tissues, which might promote development of esophageal cancer.

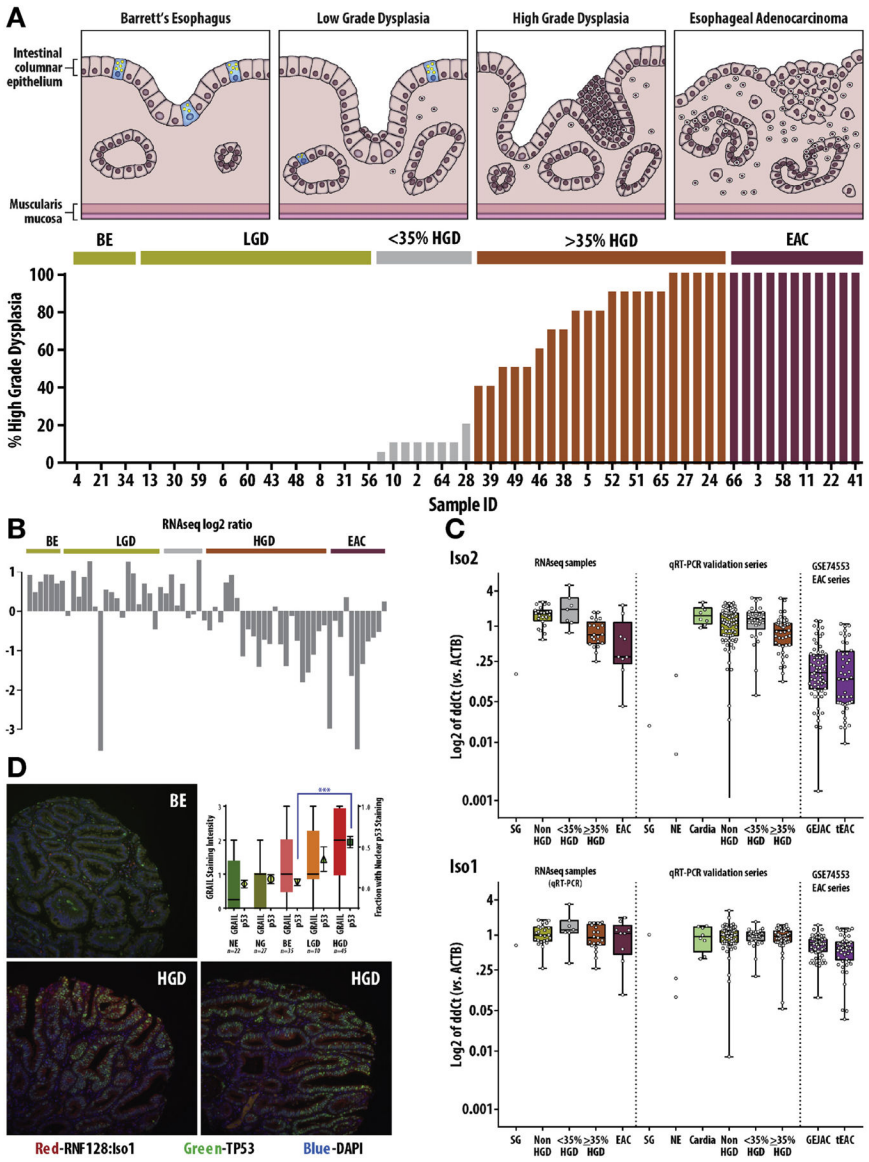

Figure 1.

RNAseq analyses of BE progression samples and isoform switching of *RNF128*. (*A*, *top*) Representative histological changes during progression of BE to EAC including loss of mucin-producing goblet cells. *Bottom* shows 65 BE samples organized by increasing dysplasia content: nondysplastic BE (n = 6), a mixture of BE and LGD with no evidence of HGD (n = 19), increasing HGD percentage (n = 29), and EAC (n = 11). (*B*) RNAseq log2 ratio of RPKM expression values for Iso2/Iso1 from *RNF128* showing lower relative Iso2 expression in HGD/EAC samples compared to BE/LGD samples ($P = .000027$; Welch test). (*C*) Quantitative reserve-transcription polymerase chain reaction (qRT-PCR) expression (ACTB as reference) of *RNF128* Iso2 and Iso1 examined in the RNAseq cohort, a larger validation cohort (n = 154 BE samples), and a cancer cohort (GEO series GSE74553) of EACs including those adenocarcinomas arising at (GEJAC), or above (tEAC) the gastroesophageal junction. (*D*) Analysis of RNF128 and TP53 protein expression examined

by Automated Quantitative Immunofluorescence Analysis (AQUA) using a BE/HGD TMA showing strong correlation between Iso1 and TP53 nuclear protein.

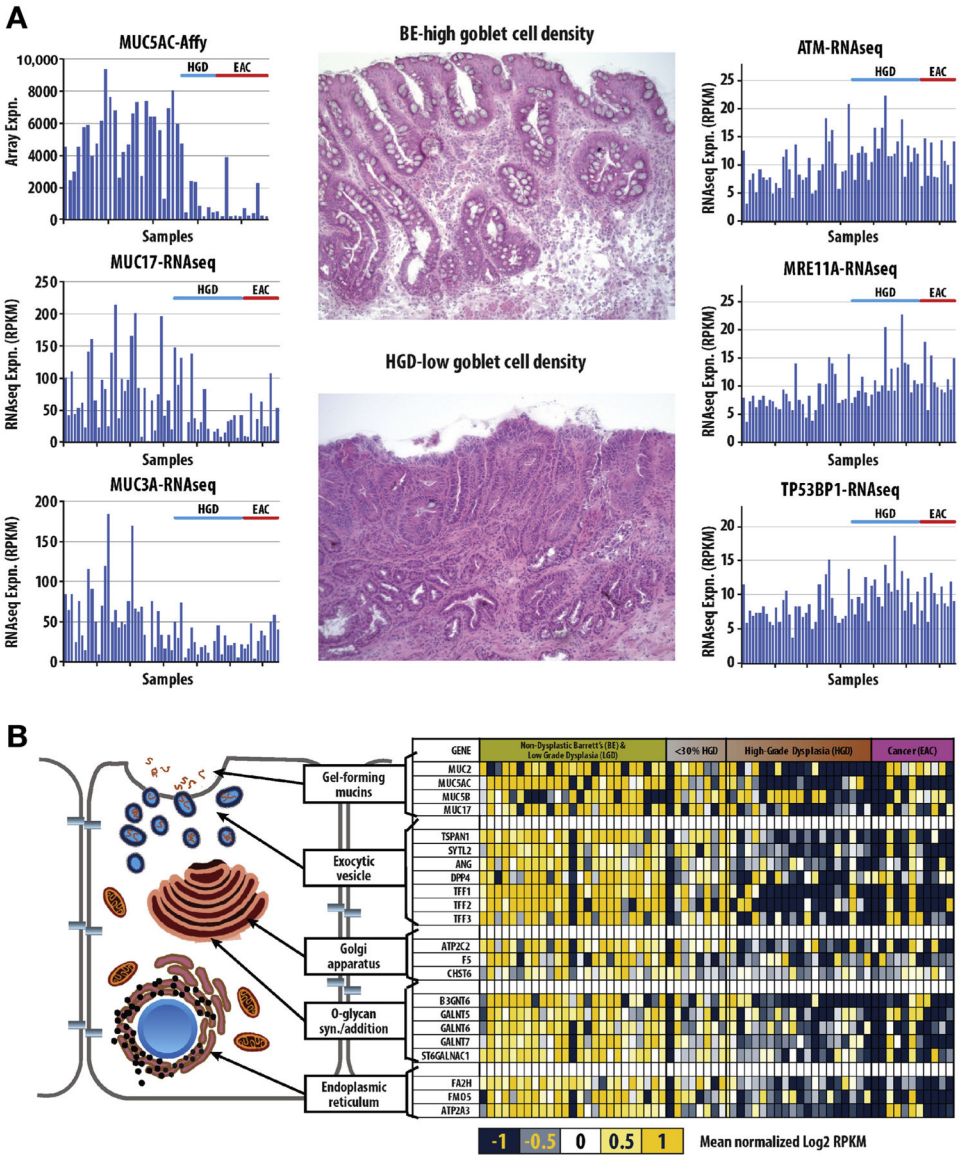

Figure 2.

Mucin loss and increased DNA damage response during BE progression. (*A*) RNAseq and Affymetrix analyses reveal loss of secreted mucin gene expression is associated with an increase in the expression of DNA damage response genes. Both BE/LGD/HGD/EAC cohorts are similarly ordered as shown in Figure 1A by increasing dysplasia content. Central images show hematoxylin-eosin staining of nondysplastic BE (*top*) and HGD (*bottom*), illustrating the complete loss of goblet cells in HGD. (*B*) Graphical representation of processes involved in mucin production and heatmap of corresponding gene expression from the RNAseq BE progression dataset.

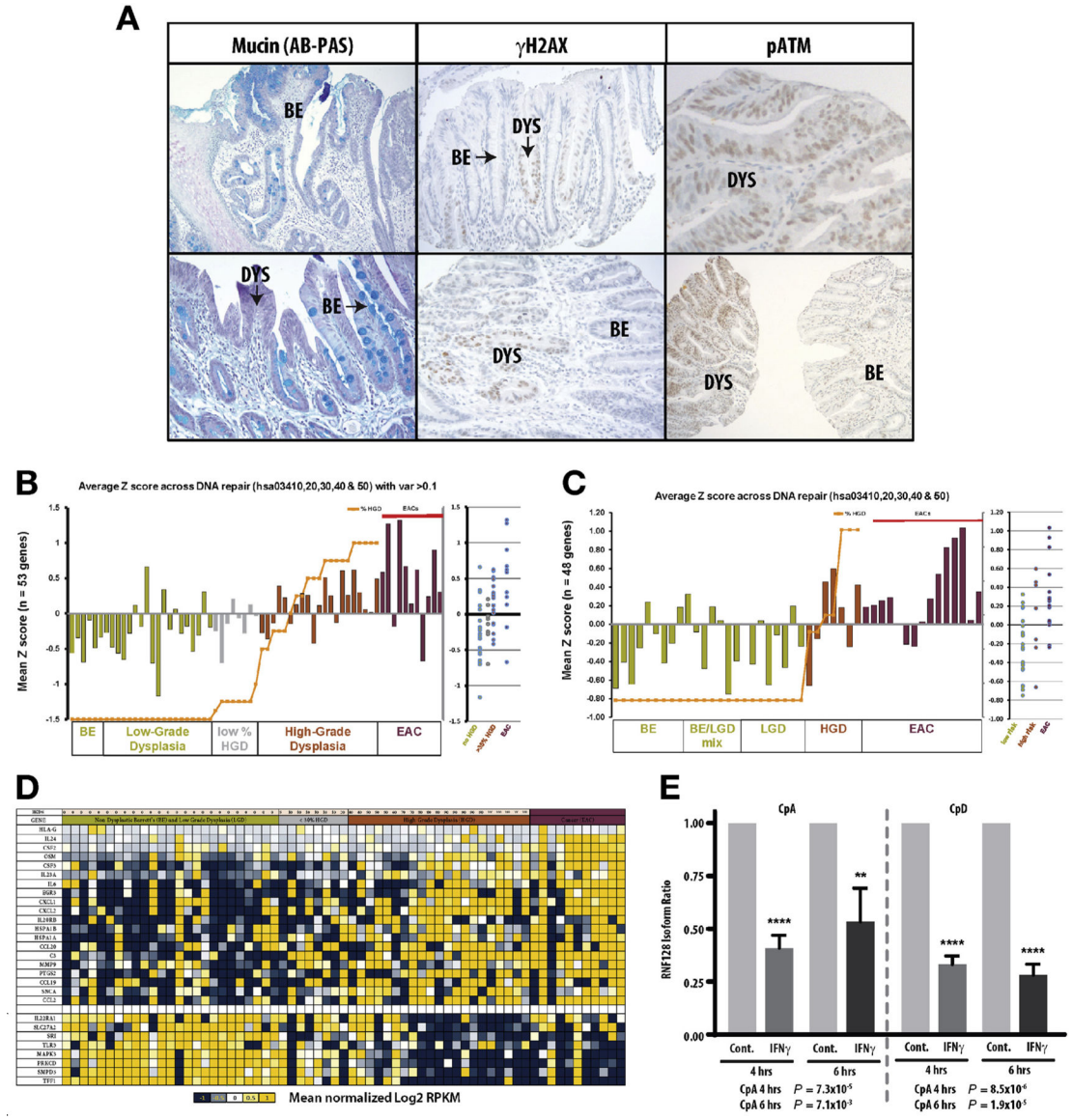

Figure 3.

Loss of mucins is associated with DNA damage as assessed by γH2AX and increased pATM expression in dysplastic BE. (*A*) Histological sections containing nondysplastic (BE) and adjacent areas of dysplasia (Dys) stained for mucin (*bright blue*) and γH2AX staining (*brown*) showing dysplastic BE regions devoid of mucin are γH2AX positive. Increased pATM protein staining in HGD relative to nondysplastic BE tissue consistent with increased ATM mRNA levels in HGD shown in Figure 2A. (*B*) *Z*-scores of RNAseq and (*C*) Affymetrix BE progression samples examined for DNA damage response genes (all 5 Kyoto Encyclopedia of Genes and Genomes pathways combined; hsa03410–50) showing and increased gene expression in HGD/EAC relative to BE/LGD. IFNγ-regulated genes during BE progression and the effect of IFNγ treatment on *RNF128* isoform expression in BE cells. (*D*) Heatmap of IFNγ-regulated genes that are either up- or downregulated during

progression of BE to EAC. (*E*) Effect of 4- and 6-hour IFNγ treatment on the isoform ratio of *RNF128* in CpA and CpD cells.

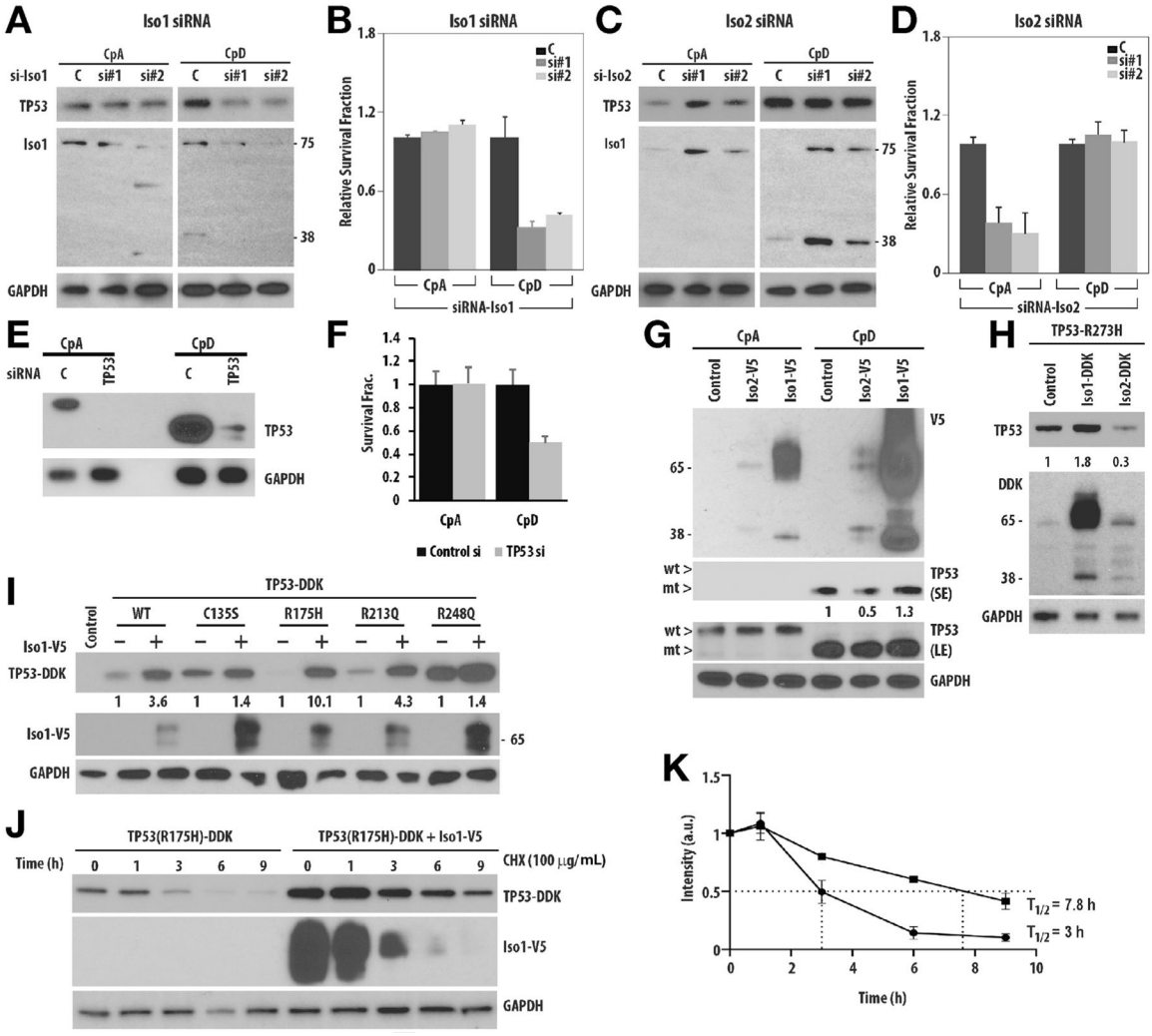

Figure 4.

Differential effects of Iso1 and Iso2 on TP53 and TP53* and clonogenic survival of BE cells. Two independent Iso1-specific siRNA transfections in CpD cells reduced TP53* levels (*A*), causing reduction in clonogenic survival (*B*). Similar Iso1 knockdown had minimal impact on TP53 containing CpA cells. (*C* and *D*) siRNA-mediated knockdown in Iso2 increased TP53 levels in CpA cells and reduced survival, whereas in TP53*-driven CpD cells, limited impact was noted. (*E* and *F*) siRNA-mediated *TP53* knockdown reduced both TP53 (CpA) and TP53* (CpD), but only CpD cells showed TP53* dependency. (*G* and *H*) Overexpression of either Iso1 or Iso2 differentially impacted TP53*; Iso2 downregulated, whereas Iso1 increased TP53* levels both in CpD and HEK293 cells overexpressing TP53* (R273H). (*I*) Iso1 overexpression increased steady-state level of TP53 and various TP53* (C135S, R175H, R213Q, and R248Q). (*J* and *K*) Half-life study using cycloheximide showed increased stability of $TP53^{R175H}$ mutant in the presence of Iso1.

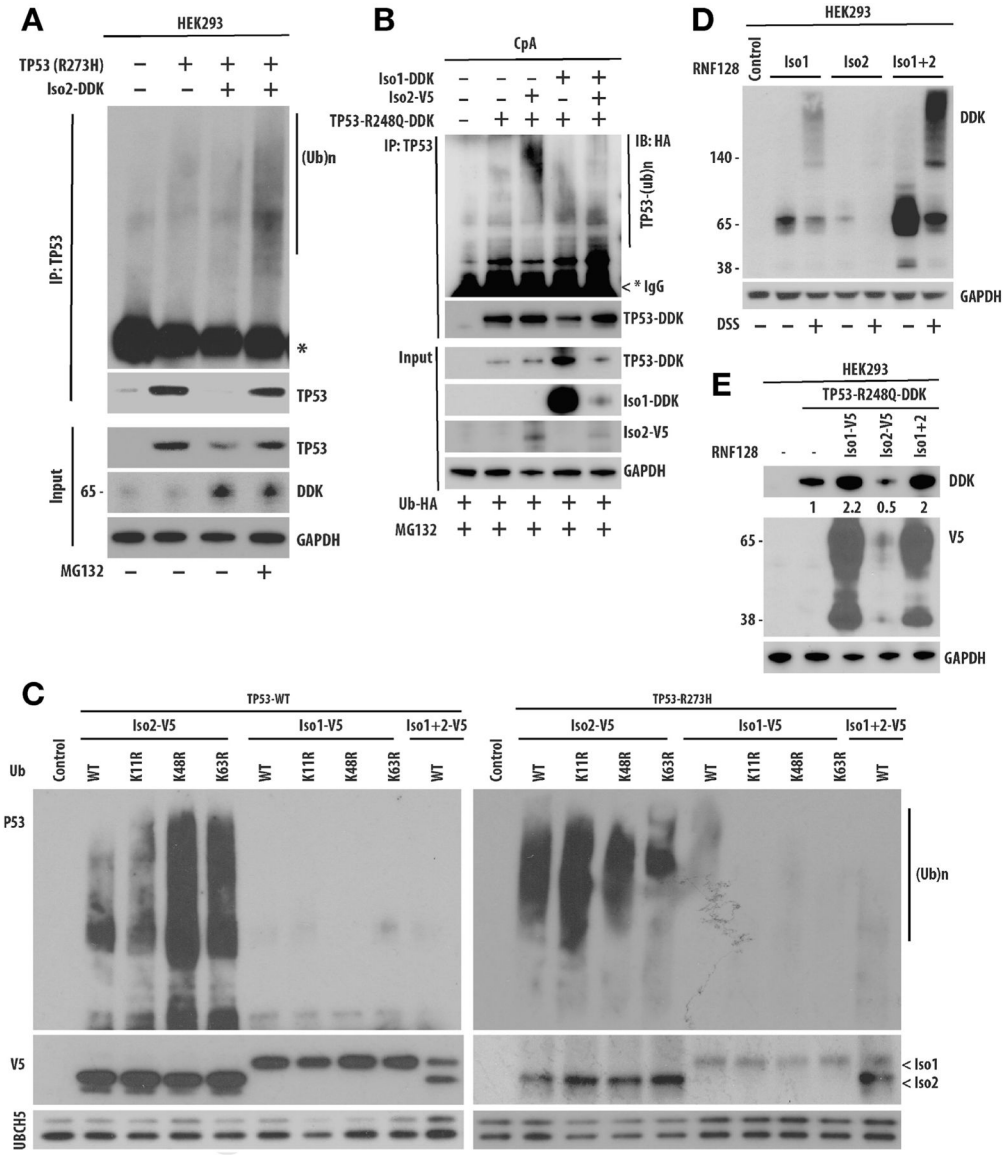

Figure 5.

Iso1 has limited ubiquitin ligase activity, whereas Iso2 efficiently polyubiquitinates and degrades TP53*. (*A*) Co-overexpression of Iso2-DDK and TP53^{R273H} in HEK293 cells promotes TP53* downregulation, and inhibits using MG132 to accumulate poly-ubiquitinated TP53*. (*B*) In contrast, Iso1-DDK overexpression inhibited Iso2-mediated TP53^{R248Q} polyubiquitination. (*C*) In a *cell-free* ubiquitination assay, in vitro transcribed and translated Iso2-V5 efficiently polyubiquitinates both TP53^{wt} and TP53^{R273H}; however, Iso1-V5 showed limited ubiquitin ligase activity. Using different ubiquitin mutants (K11R, K48R, and K63R), Iso2 attached different Ub linkages on TP53 and TP53*. Importantly, the presence of Iso1 significantly reduced Iso2 poly-ubiquitination of TP53 and TP53*. (*D*) Using protein cross-linking agent DSS, Iso1 formed effective homodimers; however, Iso2 was less efficient. In contrast, Iso1-Iso2 heterodimerization was preferred, which compromises Iso2 ubiquitin ligase activity. (*E*) Following co-transfection of V5-tagged

RNF128 and DDK-tagged $TP53^{R248Q}$, although Iso1 increased and Iso2 reduced the TP53* steady-state levels, the presence of Iso1 inhibited Iso2-mediated downregulation of TP53*.

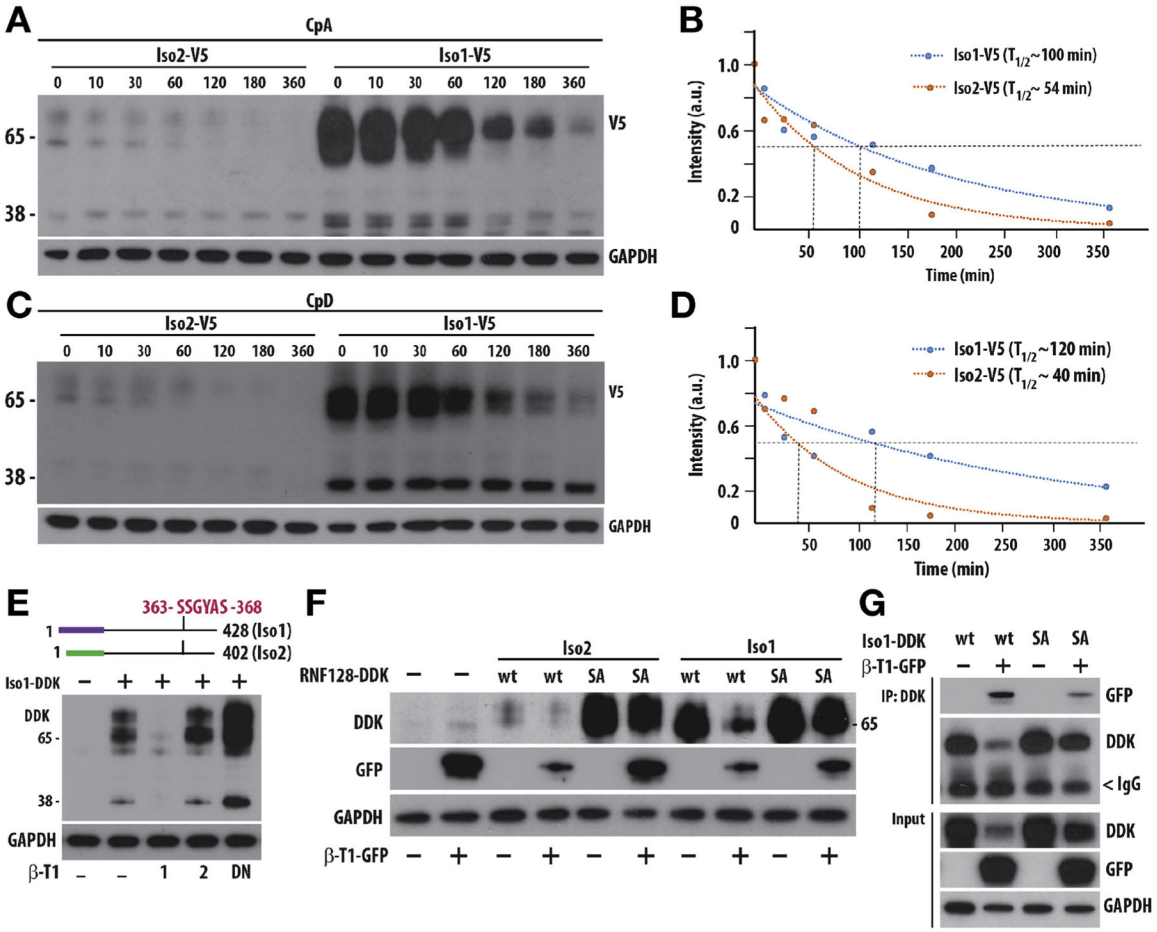

Figure 6.

RNF128 protein stability is differentially impacted by phosphorylation in an isoform-specific manner. V5-tagged Iso1 and Iso2 protein half-lives were measured in CpA and CpD cells using cycloheximide (*A* and *C*) and quantified (*B* and *D*), showing Iso1 is a more stable protein. (*E*) Probable phospho-degron (363-SSGYAS-368) in RNF128, which can be recognized by β-TrCP. β-TrCP1 overexpression but not β-TrCP2 promoted RNF128 degradation. A dominant negative (DN) form of β-TrCP1 increased RNF128 steady-state levels. (*F*) Serine-to-alanine (SA) mutants of Iso1 and Iso2 showed increased steady- state levels and were resistant to β-TrCP1-mediated downregulation, suggesting phosphorylation affects RNF128 protein stability. (*G*) SA mutant of RNF128 interacted less efficiently compared with wild type, indicating the importance of RNF128 phosphorylation in β-TrCP1 interaction.

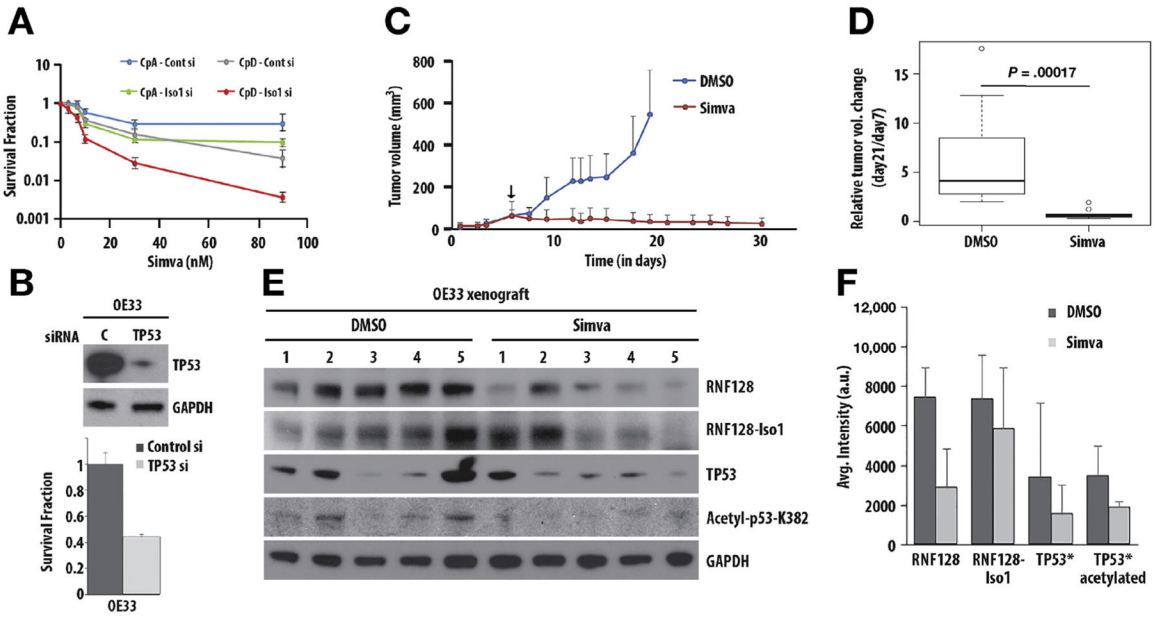

Figure 7.

Simvastatin treatment reduces RNF128 and TP53* protein levels to inhibit OE33 tumor growth. (*A*) TP53*-driven CpD cells showed increased sensitivity to simvastatin (SIM) on siRNA-mediated loss of Iso1 compared with wild-type TP53 containing CpA cells, as determined using clonogenic survival assay. (*B*) In OE33 EAC cells with TP53*, siRNA-mediated loss of TP53* resulted in reduction in clonogenic survival, showing dependency. (*C*) Simvastatin treatment inhibited tumor growth of TP53*-driven OE33 cells in nude mice compared with vehicle-treated control tumors. (*D*) Relative change in tumor volumes in days 21 and 7 post tumor detection showing statistically significant difference between vehicle- and simvastatin-treated groups. (*E*) Tumor cell lysates immunoblotted using indicated antibodies, show reduced TP53* and RNF128 (Iso1) levels in simvastatin-treated group compared with control, which was quantified as an average from 5 independent tumors (*F*).